Study of bearing fault detectability on a rotating machine by vibro-acoustic characterisation as a function of a noisy surrounding machine

Emmanuel Attal, Elga Ossonemane Asseko, Edgard Sekko, Nadia Sbai, Philippe Ravier

Study of bearing fault detectability on a rotating machine by vibro-acoustic characterisation as a function of a noisy surrounding machine

Emmanuel ATTAL[1], Elga OSSONEMANE ASSEKO[1], Edgard SEKKO[1],
Nadia SBAI[1], Philippe RAVIER[1]

[1]Univ d'Orléans, IUT de Chartres, PRISME (EA 4229), 21 rue Loigny-la-Bataille, 28000 Chartres, France
emmanuel.attal@univ-orleans.fr
philippe.ravier@univ-orleans.fr

Abstract

In a context study linked to the preventive maintenance of industrial machinery, a vibro-acoustic study aimed at identifying the defect presence in cylindrical bearings was carried out under noisy environmental conditions. The simultaneous acquisition of acoustic and vibratory signals providing information on the condition of the bearings was carried out using microphonic and accelerometric sensors positioned in close and direct contact with an engine test bench. Three types of roller bearing were studied: one with no fault and two others with different numbers of faults. The signals acquired were analysed using the RMS, Kurtosis and Talaf indicators and discussed as a function of the rotating machine speed and the signal-to-noise ratio in the time domain. The acoustic and vibration indicators are compared and analysed to assess their relevance for fault detection.

1 Introduction

Rotating machines are present on a daily basis, especially within Industry 4.0 and are widely employed in pharmaceuticals, cosmetics or nuclear power sector, to name just a few. Over time, the roller bearings used in industrial machinery will wear and lead to the appearance of faults. Roller bearings diagnosis is commonly achieved by mechanical vibration analyses. Several approaches for detecting bearing defects including vibration monitoring are widely applied [1, 2]. Other works have focused on other modalities that can reveal deficiencies of the mechanical system by inspecting acoustic emissions [3, 4, 5, 6]. Much recent vibro-acoustic experiments conducted on rotating machines bearing have proved that under some speed and load conditions with a progressive defect size increase, acoustics methods are more effective for defect detection than vibratory approaches [7, 8]. Work based on the numerical simulation of vibration signals from a machine has demonstrated the effectiveness of detecting faults in bearings using sophisticated algorithms such as demodulation, spectral kurtosis and spectral correlation [9]. Cocconcelli et al [10] also demonstrated that the use of certain statistical parameters developed by Hjorth would help to identify a certain number of defects present on ball bearings.

Simple acoustic sensors in mobile phones are sufficient to diagnose the bearings conditions [11, 12].

Based on existing databases or self-acquired signals with simulated faults created in a healthy bearing, these works conclude on the potential of combining non-invasive techniques for better classification [13, 14]. However, these studies have been carried out in laboratory environments. Indeed, real noisy operating environments may cause harm to the potential superiority of one modality with respect to the others.

Litterature review concluded that the statistical parameters can highlight indication of defect presence in bearing in their early stages and hence very useful for bearing condition monitoring [15]. These parameters depend on various factors such as defect type (inner race, outer race or rolling element defect), defect size (width and depth), shaft speed, radial load, etc.

The authors took the chances from an X-ray diffraction machine located in the same lab where some condition monitoring tests were running of a berings test rig. Since the high noise generetaed by the X-ray machine

in working conditions, its impact on the acoustic diagnostics of defective cylindrical bearings has been investigated in this paper.

We propose a preliminary study based on the statistical indicators analysis measured in time domain by both acoustic and vibration surveys. Finally, the noise increase effect product by the industrial machine on the statistical indicators evolution measured is discussed in this manuscript. This work will enable to suggest the best suited classification to the disturbing operating condition.

2 Experimental procedure

2.1 Experimental setup

The vibro-acoustic measurement chain used to characterise the state of wear of the bearings is shown in Figure 1 and 2. It consists of a Gunt PT 501 bearing fault simulator, which is composed of an asynchronous electric drive motor, a shaft with laser tachometer and a set of healthy and faulted bearings. A location has been provided for positioning of bearings on the machine. The housing has been designed to receive a load applied horizontally by the winding of a micrometer screw on a rubber compression spring mounted on its edge. The motor speed is changed by the user thanks to a rotary knob present on the device. Its value is then measured by an optical sensor which communicates to a PC via a USB interface.

Acoustic and vibration measurements are respectively performed with a cardioid microphone (type DPA 080-DC-D-B10) and an accelerometer (type A/123/TE Piezo-Tronic IEPE). In order to record acoustic and vibration responses that are most representative of the bearing conditions, these two sensors were positioned vertically and in direct contact with the bearing housing as shown in Figure 1. A sound card (type Scarlett 6i6) is used to control the acoustic inputs and outputs and allows the microphone amplification. A Compact DAQ USB chassis (National Instrument type) including a NI-9250 module ensure the timing control, synchronisation and transfer of the acoustic and vibration measurements to the PC at a sampling rate of 102.4 kHz. Finally, a LabView program allows the acoustic and vibration data acquisition.

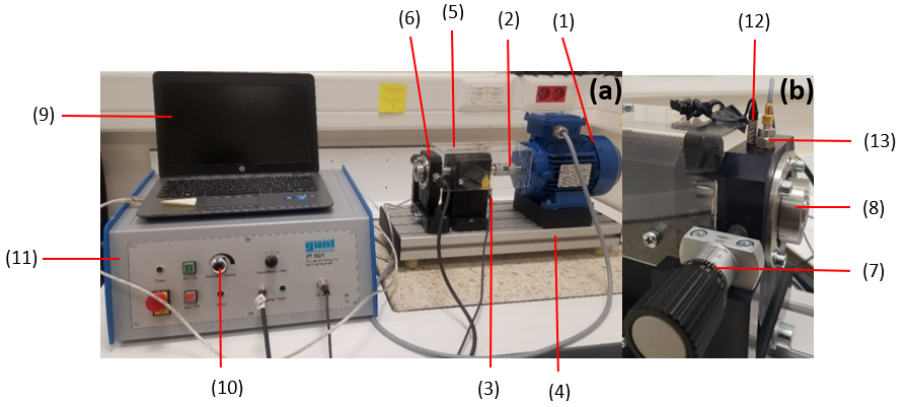

Figure 1: Vibro-acoustic characterisation device of the bearings state of wear (1) Electric Motor (2) Claw coupling (tachometer) (3) Reference transmitter for speed detection (4) Base plate for motor and support (5) Transparent cover for shaft protection (6) Bearing housing (7) Precipitating device for radial forces (8) Adjustment ring for fixing the inner race of the bearing (9) Computer for data acquisition (10) Speed adjustment knob (11) Control unit (12) Microphone (13) Non-intrusive accelerometer

2.2 Roller bearing description

The vibro-acoustic experiments were carried out on three bearings. All properties of theses bearings are given in Table 1. The first (bearing A) has no defects and is therefore the reference bearing. The second (bearing B) presents damage to the outer ring. The third (bearing E) has 3 defects which are located on the outer and inner ring and on the rolling element. A view of all these bearings is shown in Figure 3.

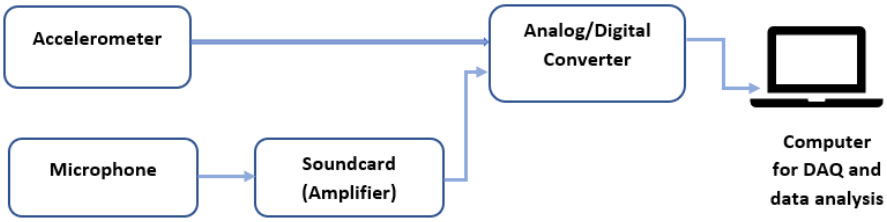

Figure 2: Schematic view of the experimental setup

Label of the bearing	A	B	E
Type of damage	No damage	Outer race	Outer race, Inner race and Rolling element

Table 1: Example of acoustic and vibratory time representations recorded on bearing B

2.3 Measurement protocol

The acoustic and vibration experiments on the rolling machine were carried out simultaneously in a room that contains an X-ray diffraction machine which is in a permanent state of operation. Therefore, the residual acoustic noise from the background noise of the room and the noise of the X-ray diffraction machine was considered in our measurements.

For each bearing, the acquisition protocol for simultaneous acoustic and vibration measurements were carried out according to the following configurations:

- Acquisition time: 18s including 3s of stop dedicated to the measurement of residual noise (background noise of the part and the X-ray diffraction machine),
- Acquisition on three speeds (1000 RPM, 2000 RPM, 3085 RPM) without radial load (adjustment screw at 0mm),
- Repeatability of measurements, by performing 3 measurements at the same environmental conditions, per speed without loads.

A total of 9 batches of measurements without radial load is thus obtain (three measurements at 1000 RPM, three at 2000 RPM and three at 3085 RPM). Note that a batch of measurements includes a vibration measurement and an acoustic measurement, which is equivalent to a set of 18 measurements per bearing.

3 Signal processing methodology

The acoustic and vibration measurements of each cylindrical bearing were processed in the same way regardless of the machine's operating speed (1000 RPM, 2000 RPM and 3085 RPM). Each 18-second time signal was divided into 6 sections of 3 seconds each, giving a total of 307200 samples analysed/per section. Note that the first 5 sections correspond to the signal from the rolling machine and the 6^{th} represents the measurement of background noise (noise from the X-ray diffraction machine). An example of the acoustic and vibration signals recorded is shown in Figure 4.

Based on this figure, the background noise was raised to evaluate the signal-to-noise ratios (SNR) for the acoustic and vibration components. This parameter must be considered when characterizing bearings, given that an X-ray machine is present in the room. As a remind, this parameter is calculated from Eq.1:

$$SNR = 20\log\left(\frac{\sigma_{Signal} - \sigma_{Noise}}{\sigma_{Noise}}\right) \tag{1}$$

where σ_{Signal} and σ_{Noise} are the standard deviation of the signal and of the noise respectively.

It is important to recall that machined or ground surfaces in bearings have a random distribution of asperities that are commonly described with a normal distribution function. This section summarises all statistical indi-

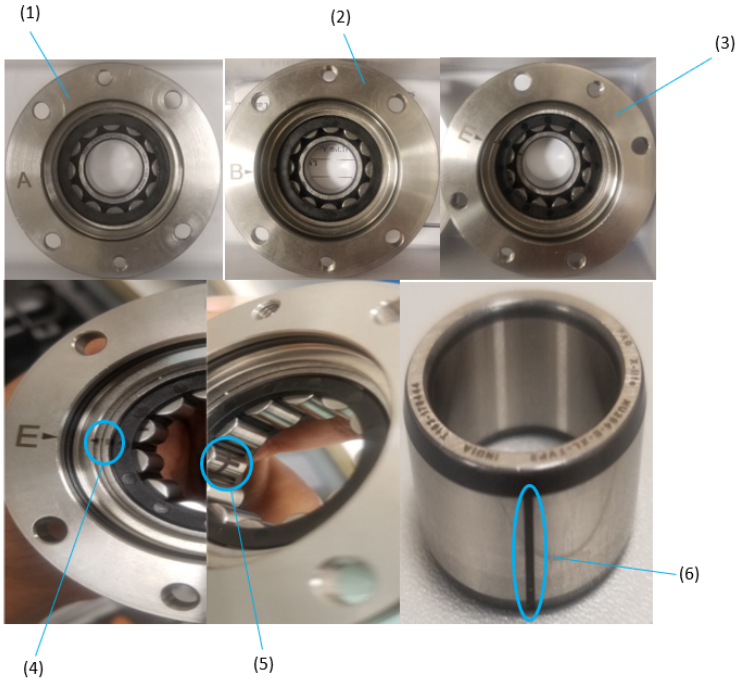

Figure 3: Details of the various bearings studied (top photos) and presence of all damage present on bearings B and E (bottom photos): (1) bearing A without damage, (2) bearing B with damage on the outer race, (3) bearing E with damage to the outer race, inner race and rolling element, (4) outer race fault, (5) rolling element fault, (6) inner race fault. (More details about the faulted bearings on the manufacturer website - www.gunt.de)

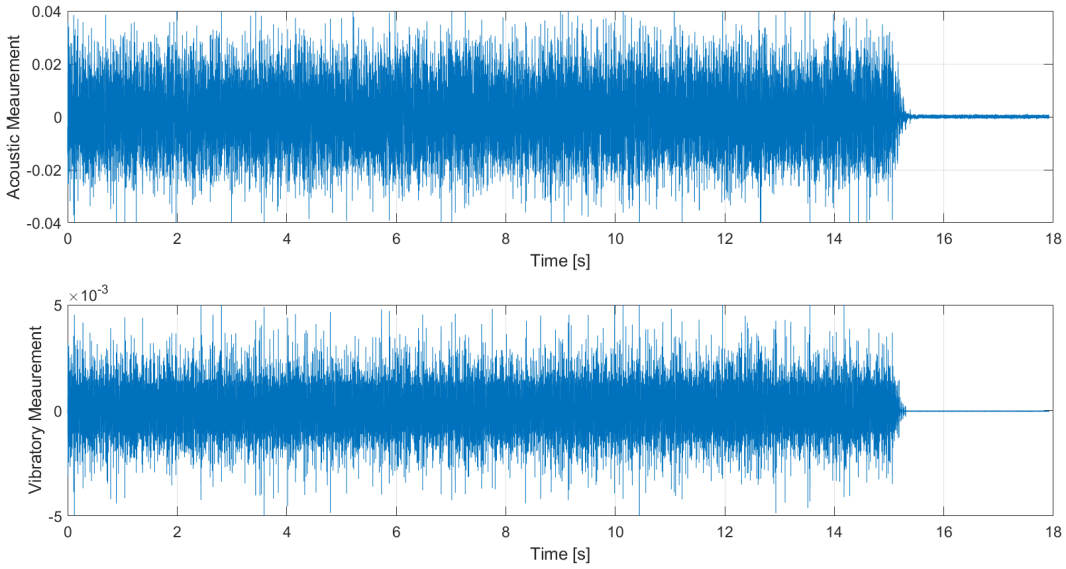

Figure 4: Example of acoustic and vibratory time representations recorded on bearing B

cators which will be used to analyse the vibro-acoustic measurements taken on cylindrical roller bearings.

The RMS value x_{RMS} is the measure of overall level of a signal (Eq.2). An excessive RMS level variation indicates a change in the operating state and therefore possibly a fault. A major limitation to be noted in the use of this indicator is that it can give a fairly late alarm, mainly in the case of bearing faults where the variation in the signal due to the appearance of the fault is masked by other components of greater amplitude.

.

$$x_{RMS} = \sqrt{\frac{1}{N}\sum_{i=1}^{N}(x_i)^2} \tag{2}$$

N is the total number of samples of the signal, x_i is the value of i^{th} sample.
Another indicator widely used to detect faults in rotating machinery is the Kurtosis $\mathscr{K}$ (Eq.3) . This indicator, which represents the impulsive nature of a signal, allows early detection of a bearing fault. A value of 3 means that the equipment is operating normally. It increases considerably as soon as impulses occur due to the appearance of a fault.

$$\mathscr{K} = \frac{\frac{1}{N}\sum_{i=1}^{N}(x_i - \bar{x})^4}{\left(\frac{1}{N}\sum_{i=1}^{N}(x_i - \bar{x})^2\right)^2} \tag{3}$$

Where $\bar{x}$ represents the mean signal.

Sassi et al [16] have developed the Talaf indicator (Eq.4) which reflects the degradation evolution from start to finish.

$$T_{ALAF} = log\left(\mathscr{K} + \frac{x_{RMS}}{x_{RMS_0}}\right) \tag{4}$$

x_{RMS} is the RMS value of a defective cylindrical bearing and x_{RMS_0} is the RMS value of a healthy cylindrical bearing.

4 Experimental results

The RMS, Kurtosis and Talaf indicators were evaluated on the basis of acoustic and vibratory measurements in order to discuss their relevance to the identification of bearing failures. Two approaches were used to interpret changes in the behaviour of each indicator:

- At constant speed and therefore varying the type of bearing,
- Same health condition of the bearing and varying the speed.

4.1 Signal-to-noise ratio assessment

The acoustic and vibration measurement quality criteria represented by the signal-to-noise ratio were raised as a function of the machine's operating regime and for each bearing, taking into account the residual noise generated by the X-ray diffraction machine and the effect of the room. The determination of this parameter is therefore essential to establish the link between the noise present in the room (independent of the bearing machine) and the detection of faults present in the bearings by acoustic and vibration measurements.

Given the number of measurements carried out for each type of bearing (three), three acoustic SNR measurements and three vibratory SNR measurements were carried out. The average SNR measurements is then deduced (Eq.5).

$$SNR_{avg} = 10\log\left(\frac{1}{M}\sum_{i=1}^{M}10^{\frac{SNR_i}{10}}\right) \tag{5}$$

where M is the number of measurements (M = 3) and SNR_i is the signal-to-noise ratio evaluated for each measurement at the same conditions. These ratios are shown in Figure 5 for the acoustic and vibration part.

In addition, these curves show that at low speeds the SNR is generally lower for the vibration measurement than for the acoustic measurement, whereas the trend is reversed at high speeds where it is the vibration measurement that gives better results (up to 52 dB for the E bearing). Noise transmitted through the ground

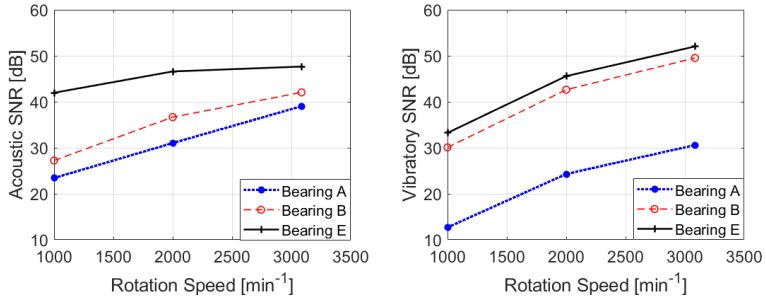

Figure 5: Acoustics and Vibratory SNRs versus rotation speed

becomes more important than that transmitted through the air. Finally, these curves show that the greater the presence of bearing defects, the better the SNR. Indeed, the absence of bearing defects results in less noise being generated by the bearing machine and, consequently, the X-ray machine channels more of the noise generated by the bearing mounted on the machine.

4.2 Measurement analysis using the RMS indicator

Figures 6 and 7 display the RMS indicator behaviour as a function of bearing type for 15 measurements taken. These results highlight that while the defect is clearly distinguishable for vibratory characterisation (red curve is closer to the black curve) at low speeds (1000 RPM), it is not as trivial for acoustic characterisation (where the blue and red curves are more closely merged).

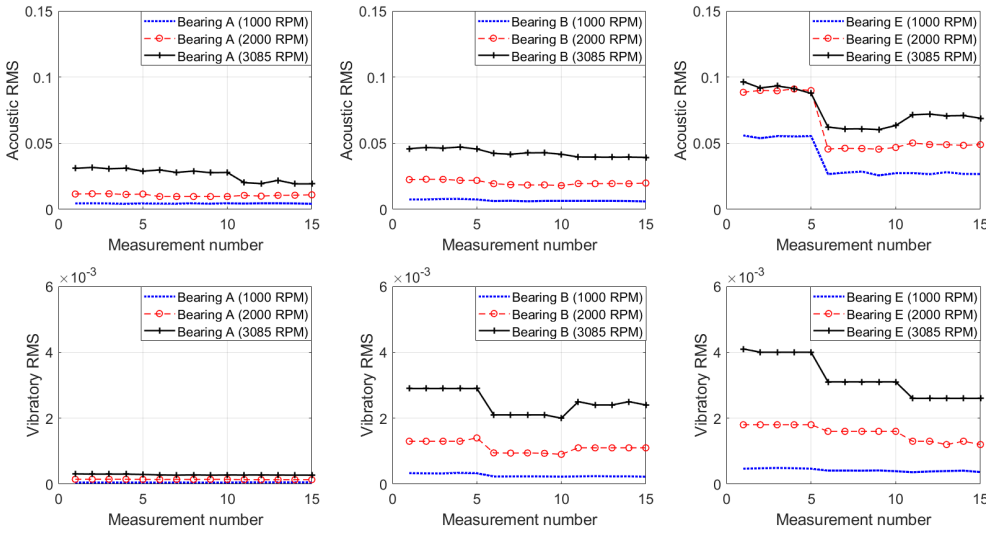

Figure 6: Acoustics and Vibratory measurement of RMS Indicator (constant bearing / variable speed)

This demarcation is confirmed as the speed increases, regardless of the method used (although the vibratory method stands out much more). Furthermore, the analysis of the amplitude scales clearly shows an amplification (by a factor of 6 for acoustic and 8 for vibratory) of the evolution in amplitude of Bearing B when going from 1000 RPM to 3085 RPM. This amplification is less obvious for bearing E, which has more defects (a factor of 2 for acoustics and vibration). Beyond a defined number of defects (bearing E), the detection sensitivity decreases and seems to increase significantly. The vibration RMS indicator stands out better overall.

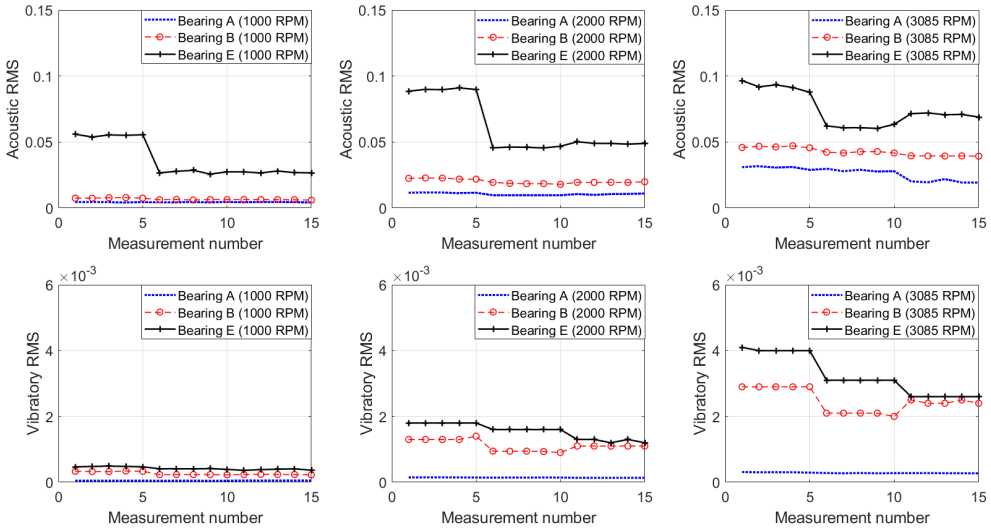

Figure 7: Acoustics and Vibratory measurement of RMS Indicator (constant speed / variable bearing)

4.3 Measurement analysis using the Kurtosis indicator

Figures 8 and 9 present the Kurtosis behaviour for the various bearings for each 15 measurement carried out as a function of the speed of rotation of the rolling bearing machine.

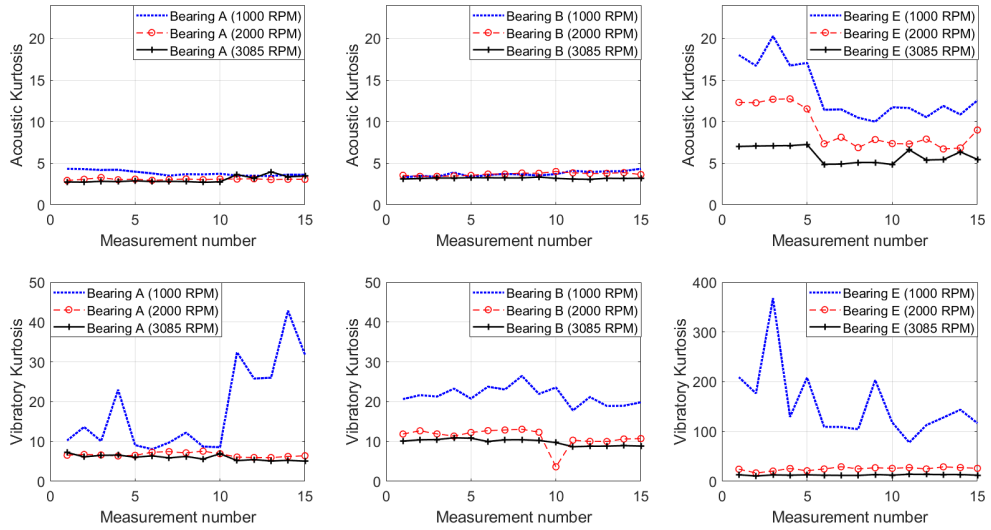

Figure 8: Acoustics and Vibratory measurement of Kurtosis Indicator (constant bearing / variable speed)

The acoustic measurements show that there is no noticeable difference between bearing A and B whatever the speed of rotation considered. Consequently, Kurtosis is unable to detect the presence of the only fault on the defective bearing B. Furthermore, the values associated with the Kurtosis of these two bearings are located around the value 3.5, which is very close to the value 3 of the normal distribution (in the case of Gaussian white noise). About the bearing E, which has 3 defects, it is interesting to note that its acoustic Kurtosis is very high at low speed (1000 RPM) and falls progressively as the rotation speed increase. It is possible to consider that at 3085 RPM the decrease compared with 1000 RPM is equivalent to a factor of 2. Consequently, the acoustic Kurtosis can only identify the presence of defects if the bearing is truly damaged. A similar analysis of the vibratory Kurtosis shows orders of magnitude greater than acoustic Kurtosis. It can also be noted that some values appear to be extremely high in the E bearing (up to 368). The vibratory trends also confirm the conclusions drawn from the acoustic part, in that the presence of a single fault is difficult to dissociate from a healthy bearing. It also appears that the Kurtosis value is the highest at low speeds and that between 2000

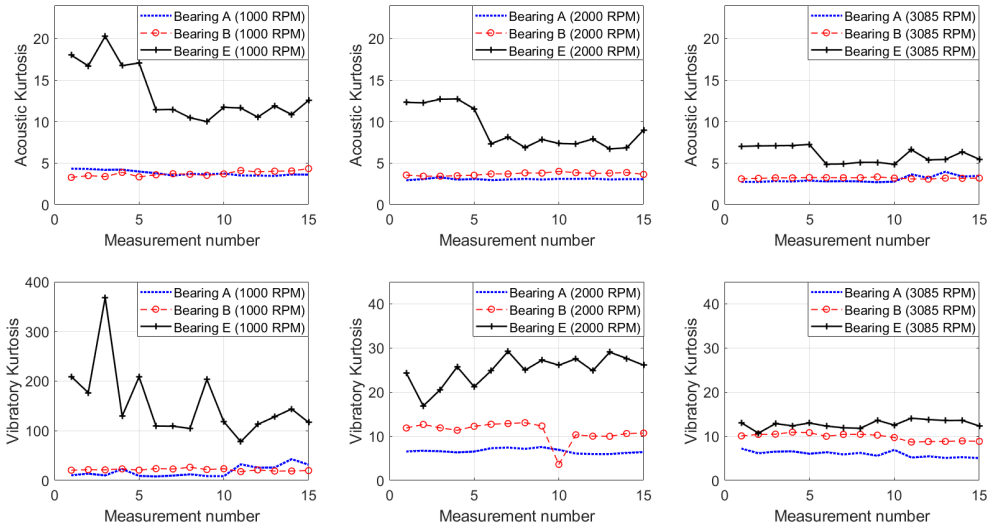

Figure 9: Acoustics and Vibratory measurement of Kurtosis Indicator (constant speed / variable bearing)

and 3085 RPM the drop in this indicator is not as obvious. Analysis of the recorded time data showed that the presence of peaks is greater at low speeds than at high speeds. This observation clearly confirms that this indicator is highly sensitive to the presence of peaks and justifies greater fluctuations. A possible explanation for this finding could be that at high revs the impact between the rolling elements is less violent than at low revs. Consequently, the spacing between each rolling element may have an impact on this result. We can therefore assume that the sensitivity of this indicator for fault detection is higher between 1000 and 2000 RPM. The observations done by Amarnath [17] on an other study of the bearings and gears condition using the acoustic Kurtosis indicator in the time domain confirm our analysis even though their measurements were taken in a quieter environment. At low speeds, the SNR is relatively low due to the predominance of the X-ray machine over the bearing machine, so it is difficult to use this indicator to detect a fault in a bearing that is only slightly defective.

4.4 Measurement analysis using the Talaf indicator

Talaf indicator evolution using the same operating conditions as previously are shown in Figure 10 and 11.

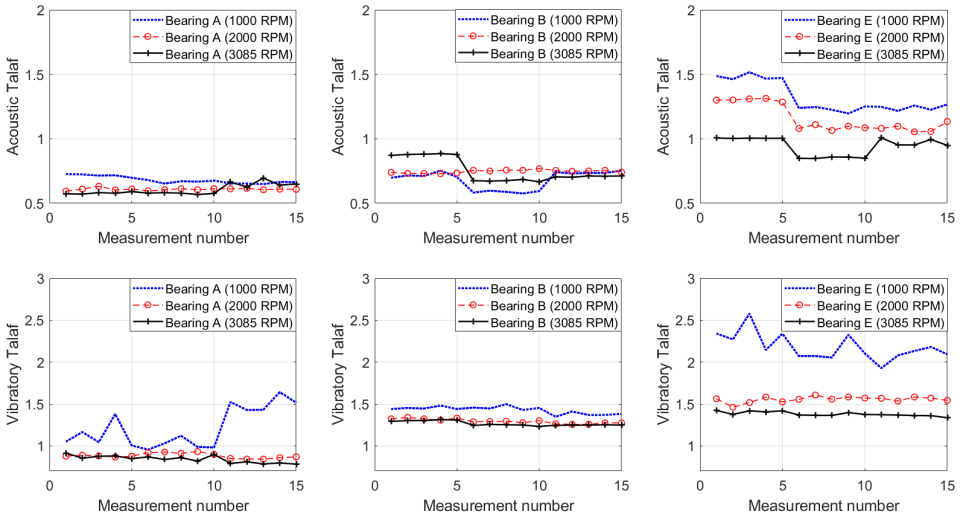

Figure 10: Acoustics and Vibratory measurement of Talaf Indicator (constant bearing / variable speed)

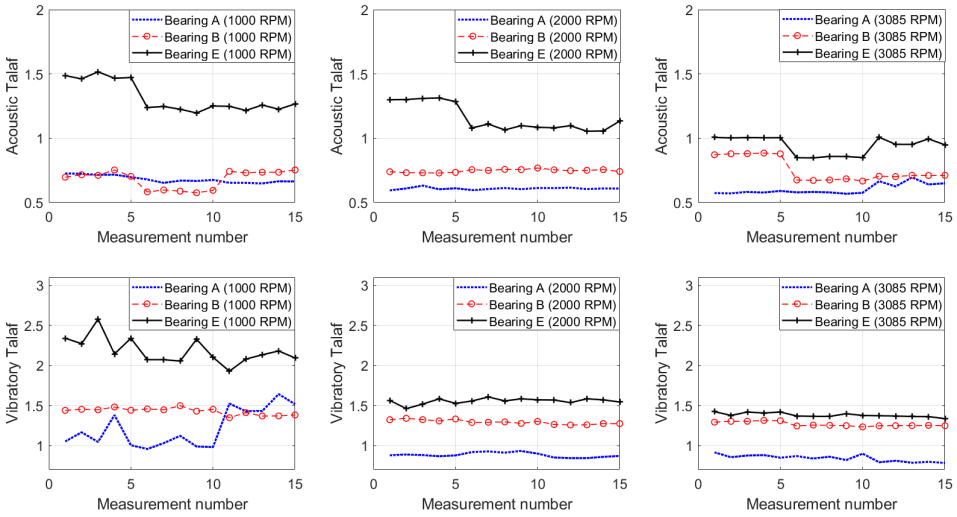

Figure 11: Acoustics and Vibratory measurement of Talaf Indicator (constant speed / variable bearing)

With regard to the Talaf indicator measured by the acoustic method, the results from Figure 10 clearly show that while the detection of the 3 failures present in bearing E (black curve) is obvious at lower speeds (1000 RPM), it is far from being so for bearing B, which only has one failure (in the outer ring).

Moreover the red curve (bearing B) tends to merge with the blue curve (healthy bearing). Curves indicate that an increase of the machine's operating speed tends to better highlight the fault presence from 3085 RPM onwards: in fact, the measurement differences between the red and the black curve tend to narrow, which means that the fault in bearing B is detected to a greater extent. On the other hand, the results obtained from the vibratory measurements in the same experimental configurations show that from 2000 RPM onwards, the distinction between a healthy and a defective bearing is much clearer than for the acoustic measurements, since this time the red and black curves are closer together.

Then, the results obtained on Figure 11 show that, for a constant bearing, an increase in the operating speed of the machine will tend to cause the value of the Talaf indicator to fall, whatever the bearing considered (healthy or defective). But the damage severity present in the bearings tends to increase the value of this indicator. The fault identification demarcation as a function of speed is clearly more noticeable in vibration analysis (where the differences between low and high speeds are substantial) than in acoustic analysis (where the differences are narrower).

5 Conclusion and outlook

We have simultaneously acquired acoustic and vibratory signals from a motor bench for two different damaged roller bearings plus one healthy. These signals were analysed in time domain using the RMS, Kurtosis and Talaf indicators and highlighted the importance of the SNR and the rotation speed of the rolling bearing machine for diagnosing the faults presence.

However, these results indicate that the vibratory testing ensures more obvious detection, as the amplitude scale becomes more distinct as the motor speed increases. Generally, indicators allow to highlight the failure impact when they are assessed at high speed (3085 RPM), where the SNR is the best (both by the acoustic and vibratory approaches).

With regard to the efficiency detection of the indicators as a function of engine rotation speed, it appears that the RMS indicator provides a better visual indication of the fault presence for the acoustic part, whatever the rotation speed or the bearing label.

The same analysis transposed to the vibratory characterization indicates that the best indicator is the Talaf, which allows a better dissociation of the bearing defect from the healthy bearing.

Vibratory results showed that due to the presence of significant peaks in bearing E measurements, the

Kurtosis displayed extremely high values at low RPM.

The outlook of this work will focus on the the impact evaluation of these indicators in the frequency domain while observing the effect of the signal window (over shorter durations). It may also involve studying the impact of the presence of other rolling defects on these indicators. A comparison of the indicators in the two fields will enable to define the one that is best suited to the treatment method used.

It could be also interesting to implement increasingly optimised methods for detecting faults at low speeds, as some authors [18] have sought to do using suitable processing methods. Finally, these indicators will be implemented in a fault classifier strategy.

6 Acknowledgments

The authors would like to express their gratitude to Marco COCCONCELLI from Modena University and Cécile CAPDESSUS for their expert advice. This work has been partially funded by Eure-Et-Loir Departmental Council.

References

[1] P.D. Mcfadden and J.D. Smith, *Model for the vibration produced by a single point defect in a rolling element bearing*. Journal of sound and vibration, vol 96(1), pp.69-82, 1984.

[2] R.B. Randall and J. Antoni, *Rolling element bearing diagnostics - A tutorial*. Mechanical systems and signal processing, vol 25(2), pp. 485-520, 2011.

[3] F. Hemmati, W. Orfali and M.S. Gadala, *Roller bearing acoustic signature extraction by wavelet packet transform, applications in fault detection and size estimation*. Applied acoustics, vol 104, pp.101-118, 2016.

[4] J.Isavand, A. Kasaei, A. Peplow, B. Afzali and E. Shirzadi. *Comparison of vibration and acoustic responses in a rotary machine balancing process*. Applied Acoustics, vol 164, pp.107258, 2020.

[5] D. Zhang, E. Stewart, M. Entezami, C. Roberts and D. Yu, *Intelligent acoustic-based fault diagnosis of roller bearings using a deep graph convolutional network, Measurement*, vol 156, 2020.

[6] B. Eftekharnejad, M.R. Carrasco, B. Charnley, D. Mba, *The application of spectral Kurtosis on Acoustic Emission and vibrations from a defective bearing*, Mechanical Systems and Signal Processing, vol 25, pp. 266-284, 2011.

[7] N.W. NIRWAN and H.B. RAMANI, *Condition monitoring and fault detection in roller bearing used in rolling mill by acoustic emission and vibration analysis*. Materials Today, vol 51, pp. 344-354, 2022.

[8] J. Grebenik, Y. Zhang, C. Bingham and S. Srivastava, *Roller element bearing acoustic fault detection using smartphone and consumer microphones comparing with vibration techniques*. 17th International Conference on Mechatronics-Mechatronika (ME). IEEE, pp. 1-7, 2016.

[9] F. Pancaldi , L. Dibiase and M. Cocconcelli, *Impact of noise model on the performance of algorithms for fault diagnosis in rolling bearings*. Mechanical Systems and Signal Processing, vol 188, pp 109975, 2023.

[10] M. Cocconcelli, M. Strozzi , J. Cavalaglio C. Molano, R. Rubini, *Detectivity: A combination of Hjorth's parameters for condition monitoring of ball bearings*. Mechanical Systems and Signal Processing, vol 164, pp 108247, 2022.

[11] M. Cakir, M.A. Guvenc and S. Mistikoglu, *The experimental application of popular machine learning algorithms on predictive maintenance and the design of IoT based condition monitoring system*. Computers & Industrial Engineering, vol 151, pp. 106948, 2021.

[12] M.S. Kolhar and N. Hiremath, *Fault Prediction of Ball Bearings using Machine Learning: A Review*. Journal of Mines, Metals and Fuels, vol 70, october 2022.

[13] J. Pacheco-Chérrez, J.A. Fortoul-Díaz, F. Cortés-Santacruz, L. María Aloso-Valerdi, D.I. Ibarra-Zarate, *Bearing fault detection with vibration and acoustic signals: Comparison among different machine leaning classification methods, Engineering Failure Analysis*, vol 139, 2022.

[14] W.N Nirwan, H.B. Ramani, *Condition monitoring and fault detection in roller bearing used in rolling mill by acoustic emission and vibration analysis*, Materials Today: Proceedings, vol 51, Part 1, pp 344-354, 2022.

[15] S. Mufazzal, S.M. Muzakkir, S. Khanam, *Enhancing the Classification Performance of Machine Learning Techniques by Using Hjorth's and Other Statistical Parameters for Precise Tracking of Naturally Evolving Faults in Ball Bearings*, International Journal of Acoustics and Vibrations, 27 (2), pp 138-150, 2022.

[16] S. Sassi, B. Badri and M. Thomas, *Tracking surface degradation of ball bearings by means of new time domain scalar indicators*. International journal of COMADEM, vol 11(3), pp 36-48, 2008.

[17] M.Amarnath and I.R. Praveen , *Empirical mode decomposition of acoustic signals for diagnosis of faults in gears and rolling element bearings*. IET Science, Measurement & Technology, vol 6(4), pp 279-287, 2012.

[18] B.Van Hecke, J. Yoon and D. He, *Low speed bearing fault diagnosis using acoustic emission sensors*. Applied Acoustics, vol 105, pp 35-44, 2016.